Available online at www.sciencedirect.com
SCIENCE DIRECT®
Biochemical Pharmacology 65 (2003) 1719–1727
Biochemical Pharmacology
www.elsevier.com/locate/biochempharm

Inflammation and inducible nitric oxide synthase have no effect on monoamine oxidase activity in glioma cells

Elizabeth Mazzio, Alan Becker, Karam F.A. Soliman*

College of Pharmacy and Pharmaceutical Sciences, Florida A & M University, Dyson Building, Room 104, Tallahassee, FL 32307, USA

Received 10 December 2001; accepted 3 October 2002

Abstract

Heightened monoamine oxidase (MAO) and inducible nitric oxide synthase (iNOS) activity can contribute to oxidative stress, the formation of active neurotoxins, and associated neurodegenerative diseases of the brain. Although these enzymes co-exist within astrocytes, there has been little research examining the correlation between the two during inflammation. In this study, C6 glioma cells were stimulated with lipopolysaccharide (LPS):*Escherichia coli* 0111:B4 (6 μg/mL):rat interferon-γ (IFN-γ) (100 U/mL). In LPS/IFN-γ-treated cells, the MAO substrates dopamine (DA) and tyramine caused a concentration-dependent attenuation of NO_2^- and NO_3^-. In contrast, treatment with an MAO-A inhibitor (clorgyline) or an MAO-B inhibitor ((−)-deprenyl) did not reverse these effects. MAO activity was inhibited effectively by clorgyline and deprenyl; however, neither MAO inhibitor had an effect on NO_2^- in stimulated cells. Inversely, increasing concentrations of LPS/IFN-γ resulted in heightened iNOS protein expression and NO_2^-; however, these events did not correlate with any distinctive change in MAO enzyme activity. Moreover, a selective iNOS inhibitor, N^6-(1-iminoethyl)-L-lysine, in LPS/IFN-γ-stimulated cells caused a concentration-dependent attenuation of NO_2^- with no effects on MAO activity or iNOS protein expression. The attenuating effects of DA on iNOS were blocked completely by ICI 118-551 [(±)-1-[2,3-(dihydro-7-methyl-1*H*-inden-4-yl)oxy]-3-[(1-methylethyl)amino]-2-butanol hydrochloride], indicating a role for the β_2-adrenergic receptor. In conclusion, these data indicate that activity or expression of iNOS does not influence MAO activity in activated rat glioma cells. Moreover, DA exerts an inhibitory effect on glial iNOS through a receptor-mediated cascade.

Keywords: Astrocyte; C6; Monoamine oxidase; Nitric oxide; Inflammation; Parkinson's disease

1. Introduction

Astroglial cells make up a large fraction of CNS cellular volume in humans, playing a predominant role in maintaining the health and viability of neurons [1]. Both MAO and iNOS are located in astroglial cells [2,3], and up-regulation of both enzymes is thought to contribute to age- or disease-related neurodegeneration of the CNS [4,5]. Although both enzyme systems contribute to the production of neurotoxins, inherently they also provide regulatory functional roles in neurotransmission. MAO is located in the outer mitochondrial membrane and is responsible for the oxidative deamination of biogenic amines and the regulation of CA neurotransmitter levels. MAO is classified into subtypes, MAO-A and MAO-B. While both enzymes are located in the CNS and exhibit similar homology, they are encoded by different genes and show different substrate and inhibitor specificities [6]. Both MAO subtypes are capable of deaminating TYR; however, MAO-A is inhibited by clorgyline and has a greater substrate affinity for serotonin and norepinephrine, whereas MAO-B is inhibited by deprenyl and has an affinity for benzylamine and DA [2,7]. NOS is located in the cytoplasm and is involved

* Corresponding author. Tel.: +1-850-599-3306; fax: +1-850-599-3667.
E-mail address: Karam.Soliman@famu.edu (K.F.A. Soliman).

Abbreviations: AD, Alzheimer's disease; CA, catecholamine; cAMP, adenosine 3′,5′-cyclic monophosphate; DA, dopamine; DMEM, Dulbecco's modified Eagle's medium; DOPAL, 3,4-dihydroxyphenylacetaldehyde; DOPEGAL, 3,4-dihydroxyphenylglycolaldehyde; FBS, fetal bovine serum; HBSS, Hanks' balanced salt solution; ICI 118-551, (±)-1-[2,3-(dihydro-7-methyl-1*H*-inden-4-yl)oxy]-3-[(1-methylethyl)amino]-2-butanol hydrochloride; IFN-γ, interferon-gamma; iNOS, inducible nitric oxide synthase; LPS, lipopolysaccharide; MAO, monoamine oxidase; NIL, N^6-(1-iminoethyl)-L-lysine, hydrochloride; NO_2^-, nitrite; NO_3^-, nitrate; $^{\bullet}OH$, hydroxyl radical; $ONOO^-$, peroxynitrite; PD, Parkinson's disease; Tris, tris(hydroxymethyl)aminomethane hydrochloride; TTBS, Tris-buffered saline containing 0.05% Tween 20; and TYR, tyramine.

0006-2952/03/$ – see front matter
doi:10.1016/S0006-2952(03)00148-5

primarily with the regulation of immune function, second messenger systems, memory, learning, pain, and neurotransmitter release [3,8,9]. NOS exists as three different isoforms, including cNOS and eNOS (constitutive forms) and iNOS (inducible form). In addition to MAO, astrocytes also contain iNOS (NOS-2), which is Ca^{2+}-independent and regulated through induction by bacterial LPS and cytokines [3].

The toxicity of MAO or NOS varies with the type of end product released. For example, NOS-2 releases NO, which can rapidly form toxic oxidative species including $ONOO^-$ and $^\bullet OH$ that can rapidly bind to heme groups [10], cause ADP ribosylation of proteins [11], and irreversibly inhibit cytochrome *c* oxidase of the electron transport chain [12]. MAO toxicity stems from the oxidative deamination process of amines, which can result in the production of toxic compounds including H_2O_2, ammonia, and aldehydes [13–15]. H_2O_2 in conjunction with transition metals such as copper or iron can generate $^\bullet OH$, which can destroy lipid and protein structural cellular components rapidly [16,17]. MAO can also metabolize DA into DOPAL and DOPEGAL, which can react with H_2O_2 to form $^\bullet OH$ [18,19]. Accumulation of DOPAL, DOPEGAL, and $^\bullet OH$ is thought to contribute to the neurodegeneration of dopaminergic neurons associated with PD [18,20]. MAO-derived aldehyde metabolites are extremely lethal because they are directly cytotoxic, and can propel the formation of free radicals or undergo condensation reactions with DA to form endogenous isoquinoline neurotoxins such as *N*-methyl(*R*)salsolinol [21,22]. Blocking either iNOS or MAO-B with selective inhibitors such as deprenyl or NIL is effective in preventing the formation of endogenous neurotoxins and in ameliorating pathologically related conditions of the CNS [22,23].

While these enzymes are localized within the same cell, there are meager data investigating their interaction during inflammation. Further, MAO is responsible for degradation of noradrenaline and 5-hydroxytryptamine, which have inhibitory effects on iNOS in glial cells [24,25]. Therefore, the aim of this study was to analyze the relationship between iNOS and MAO during bacterial endotoxin/cytokine activation in glioma cells.

2. Materials and methods

2.1. Materials

Rat C6 glioma cells were obtained from the American Type Culture Collection. DMEM, L-glutamine, heat-inactivated FBS, PBS, HBSS, and penicillin/streptomycin were supplied by Fischer Scientific, Mediatech. Tris (10×)/glycine buffer, SDS buffer, Laemmli sample buffer, gels, and 0.2 μM nitrocellulose were purchased from Bio-Rad. Rat IFN-γ was obtained from Gibco, and all other chemicals and supplies were purchased from the Sigma Chemical Co.

2.2. Cell culture

C6 glioma cells were grown in phenol red-containing DMEM supplemented with 10% (v/v) FBS, 4 mM L-glutamine, and penicillin (100 U/mL)/streptomycin (0.1 mg/mL). The cells were grown at 37° in a 5% CO_2 in air atmosphere, and cells were trypsinized (0.25% sterile trypsin/0.02% EDTA in HBSS) and subcultured every 2–5 days. Experimental plating medium consisted of DMEM minus phenol red, 1.8% (v/v) FBS, penicillin (100 U/mL)/streptomycin (0.1 mg/mL), and 4 mM L-glutamine. Cells (100 μL) were plated at approximately 1.0×10^6/mL in 96-well plates. A stock solution of each experimental compound was prepared in HBSS + 10 mM HEPES and adjusted to a pH of 7.4. Six concentrations of each experimental compound were prepared in buffered HBSS to span a 1000-fold experimental dilution range.

2.3. MAO

MAO activity was determined by a modification of a previous method [26]. MAO is located in the mitochondrial membrane; therefore, generating a cell lysate is required for quantification of enzyme activity. After storage at −80° for 48 hr, samples were brought to room temperature by slow thawing. Previous data from our laboratory indicate that the use of protease inhibitors (such as 5 μg/mL of aprotinin, pepstatin A, or leupeptin) or sodium azide (from 1 mM to 1 μM) in the lysate buffer had no effect on signal/product ratio (unpublished data). Therefore, protease inhibitors or azide were not used. The substrate (10 μM–10 mM TYR, final concentration) was prepared in PBS + 3 mM HEPES and adjusted to pH 7.4. The substrate solution was added immediately to the cell lysate during thawing. After addition of the substrate, the chromogenic reagent was added [final concentration: 1 mM vanillic acid, 500 μM 4-aminoantipyrine, and Type II horseradish peroxidase (4 purpurogallin units/mL)] in buffered PBS. Samples were vortexed gently and returned to the incubator for timed continuous experiments. Data were quantified at 490 nm on a UV microplate spectrophotometer (model 7600, version 5.02, Cambridge Technologies Inc.). Controls and blanks were run simultaneously, and subtracted from the final value to eliminate interference. Protein was assessed by the method of Lowry *et al.* [27], and data were expressed as pM product formed (H_2O_2)/mg protein/min or percent of control.

2.4. NO_2^-/NO_3^-

Quantification of NO_2^- was determined by a colorimetric method using the Griess reagent [28]. The Griess reagent was prepared by mixing an equal volume of 1.0% sulfanilamide in 0.5 N HCl and 0.1% *N*-(1-naphthyl)-ethylenediamine in deionized water. At the end of the experimental period, sample NO_3^- was converted to NO_2^- by the addition

of an enzyme solution prepared in buffered HBSS, pH 7.4, containing nitrate reductase (EC 1.6.6.1) (0.2 U/mL), 0.5 μM EDTA, 2.5 mM 3-[*N*-morpholino]-propanesulfonic acid, 0.05 mg/mL of BSA, and 100 μM NADH. For the quantification of total NO_3^-/NO_2^-, the nitrate reductase solution was added directly to the samples. For the determination of NO_2^-, an equal volume of buffer without the enzyme was added to each sample. Subsequently, samples were vortexed gently and incubated simultaneously at room temperature for 25 min. The Griess reagent was added directly to the cell supernatant suspension and incubated under reduced light at room temperature for 10 min. An NO_3^- standard curve containing buffer ± nitrate reductase was run in parallel to ensure conversion of NO_3^- to NO_2^- in 25 min. A standard curve for NO_2^- was generated from dilutions of sodium nitrite ($NaNO_2$) (1–100 μM) prepared in plating medium. Controls and blanks were run simultaneously, and subtracted from the final value to eliminate interference. Samples were analyzed at 550 nm on a UV microplate spectrophotometer (model 7600, version 5.02, Cambridge Technologies Inc.). Protein was assessed by the method of Lowry *et al.* [27], and data were calculated as nM NO_2^-/mg protein or percent of control.

2.5. Cell viability

Resazurin (Almar blue) indicator dye was used as a measure of viable cell count. The use of this dye has been established as a rapid protocol for toxicity testing, with advantages in specificity, repeatability, low probability of cross-reactivity or false positive identification, and a high correlation to *in vivo* toxicity [29]. Briefly, a working solution of resazurin was prepared in PBS minus phenol red (0.5 mg/mL). Reduction of the dye by viable cells reduces the amount of the oxidized form and increases the amount of its bright red fluorescent intermediate (resorufin). The dye solution was added [15% (v/v) equivalent] to the culture medium. Cultures were returned to the incubator for 6–8 hr. Controls and blanks were run simultaneously, and subtracted from the final value to eliminate interference. Quantitative analysis of dye conversion was measured on a microplate fluorometer (model 7620, version 5.02, Cambridge Technologies Inc.) set at an excitation wavelength of 550 nm and emission wavelength of 580 nm. Data were expressed as percent of the live control.

2.6. Western blotting

Western blot analysis was done with minor modifications from a previous method [30]. After experimental treatment, the supernatant for each sample was removed and discarded. The cell monolayer was washed with PBS and placed in a lysis buffer. The lysis buffer consisted of 5% glycerol, 1 mM sucrose, 200 μM phenylmethylsulfonyl fluoride, 10 mM Tris, 5 μg/mL of pepstatin A, 1 mM EDTA, 10 μg/mL of aprotinin, 10 μg/mL of leupeptin, 2 mM DL-dithiothreitol and 3 M urea prepared in 18 MΩ water. Samples were stored at −80° for 24 hr and lysed by freeze–thaw. The cell lysate was placed in Laemmli sample buffer with 3.0% 2-mercaptoethanol. Samples were boiled for 5 min and centrifuged at 13,000 *g* for 5 min at room temperature. The supernatant was removed for western blot and protein analysis. Protein was assessed using the method of Lowry *et al.* [27].

Proteins were separated on a 10% SDS–polyacrylamide gel using the Laemmli buffer system and transferred to nitrocellulose at 125 V for 1 hr in Towbin-SDS transfer buffer containing 25 mM Tris, 192 mM glycine, and 20% methanol. After transfer, the blot was washed once with TTBS. For rapid determination of iNOS, a new rapid 2-hr protocol for immunostaining was developed by R & D Systems. Briefly, the blot was dried thoroughly. The 1° antibody used was specific for iNOS (macNOS) and was developed in rabbits using the synthetic peptide FSYGAKKGSALEEPKATRL corresponding to the C-terminus of iNOS of mouse macrophage origin (amino acids 1126–1144) conjugated to keyhole limpet hemocyanin as the immunogen. This sequence is highly conserved in rat macNOS. Whole antiserum was fractionated and then further purified by ion exchange chromatography to provide the immunoglobulin G (IgG) fraction of antiserum that was free of other rabbit serum proteins (Sigma). The 1° antibody was diluted 1:6000 in a diluent buffer containing 1% BSA (Fraction V) in TTBS and 0.2% sodium azide. Twenty milliliters of diluted 1° antibody was added to the membrane and incubated on a rocker/shaker at room temperature for 1 hr. The membrane was washed, and 20 mL of diluted 2° antibody [anti-rabbit IgG (whole molecule) peroxidase conjugate; 1:4000] was added and incubated on a rocker/shaker at room temperature for 1 hr. After a final wash, peroxidase was detected with SIGMA FAST™ DAB (3,3′-diaminobenzidine tetrahydrochloride) with a metal enhancer, $CoCl_2$.

2.7. Data analyses

Statistical analysis was performed using Graphpad Prism (version 3.0), Graphpad Software Inc. Data were expressed as the means ± SEM for each group. The significance of difference between the treated and the control was assessed using a one-way ANOVA, followed by a Tukey post hoc means comparison test. Significance of difference between groups was assessed by a two-way ANOVA.

3. Results

The effect of MAO substrates, TYR and DA, on iNOS were evaluated (Fig. 1a and b, respectively). C6 glioma cells were pretreated with experimental compounds for 2 hr prior to treatment with LPS:*Escherichia coli* 0111:B4

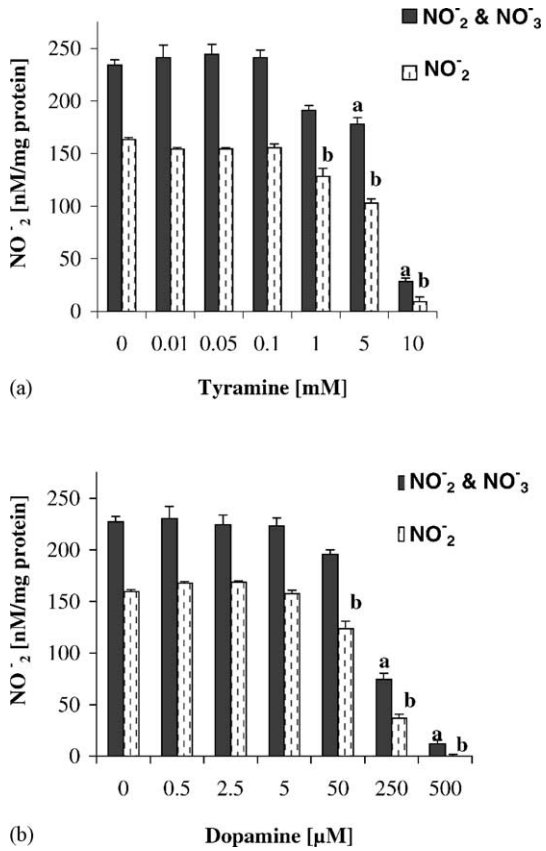

Fig. 1. Effect of MAO substrates on LPS/IFN-γ induction of iNOS: quantification of NO_2^-/NO_3^-. Data represent NO_2^- [nM/mg protein], and are expressed as means ± SEM, N = 4. Significance of difference from the control was determined by a one-way ANOVA, followed by a Tukey mean comparison post hoc test (NO_2^-/NO_3^-). Key: (a) $P < 0.001$ (NO_2^-), (b) $P < 0.001$.

(6 μg/mL):IFN-γ (100 U/mL). Samples were returned to the incubator for 24–36 hr at 37° in a 5% CO_2 in air atmosphere. The tests were monitored with timed controls, to ensure that a desired level of NO_2^- production had been achieved. The concentration of [NO_2^- and NO_3^-]/[NO_2^-] in the treated controls reached a value of [234.1]/[163.4] nM NO_2^-/mg protein. Baseline controls produced [21.4]/[3.79] nM NO_2^-/mg protein (data not shown). With slight effects on cell viability (Fig. 2), TYR and DA caused a parallel and concentration-dependent inhibition of [NO_2^- and NO_3^-]/[NO_2^-], $P < 0.001$. To determine if the effects of substrate inhibition were due to the dissipation of NO_2^- directly or Griess reagent reactivity, TYR and DA were incubated for 24 hr, in experimental plating medium with $NaNO_2$ (20 μM) (Fig. 3). Due to the effects of acid on DA optical absorbance (550 nm), a control was established to quantify and subtract any reduction observed with an equal volume of 0.5 N HCl and DA. There were no attenuating effects of DA or TYR on Griess reagent reactivity or interaction with $Na^+NO_2^-$. Since both quantitative assays for MAO and NOS require chromogenic detection of reactive oxygen species, a quality control test for cross-reactivity was done, and the data indicated that the methods were specific and accurate (data not shown). H_2O_2 was not detected with the Griess reagent, and sodium nitroprusside (NO donor) was not detected with vanillic acid and 4-aminoantipyrine condensation. Figure 4 demonstrates MAO activity and NO_2^- concentration in LPS/IFN-γ-stimulated cells in the presence of clorgyline and deprenyl. Clorgyline and deprenyl caused a concentration-dependent inhibition of MAO (from 100 ± 1.8 to 2.9 ± 1.7% and from 100 ± 2.4 to 0 ± 1.5%, respectively); $P < 0.001$, respectively. However, neither MAO inhibitor had any effect on NO_2^- levels. To further corroborate a lack of interconnectedness between the two enzyme systems, iNOS protein expression and NO_2^- were quantified using various concentrations of LPS/IFN-γ with NIL as a negative control (Fig. 5). Figure 5 shows a concentration-dependent increase in iNOS enzyme and NO_2^- with increasing concentrations of LPS/IFN-γ (right). NIL was

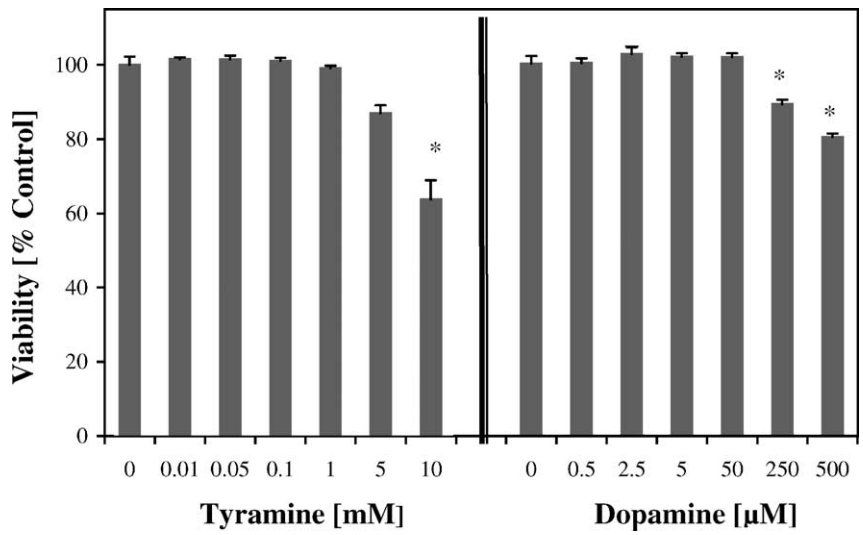

Fig. 2. Effects of MAO substrates + LPS/IFN-γ on C6 cell viability. Data represent viability [% control], and are expressed as means ± SEM, N = 4. Significance of difference from the control was determined by a one-way ANOVA, followed by a Tukey mean comparison post hoc test. Key: (*) $P < 0.001$.

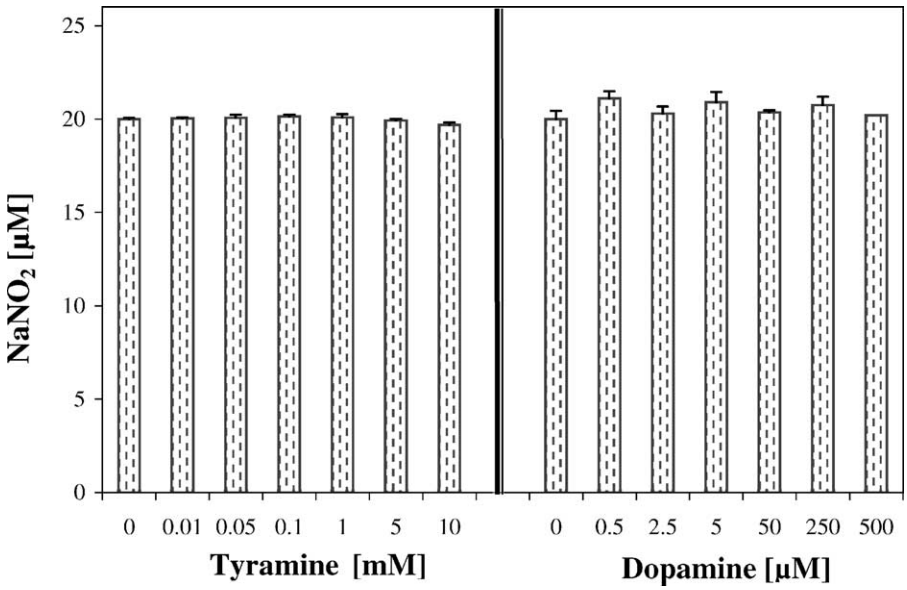

Fig. 3. Effects of MAO substrates on potential Griess reagent or $NaNO_2$ (20 μM) cross-reactivity. Data represent $NaNO_2$ [μM] remaining after 24 hr of incubation, and are expressed as means ± SEM, N = 4. Significance of difference from the control was determined by a one-way ANOVA, followed by a Tukey mean comparison post hoc test. There were no significant differences (NS).

effective in reducing NO_2^-, with no effect on iNOS protein expression (left). In Fig. 6, MAO activity was analyzed under the conditions presented in Fig. 5. MAO activity using 1 mM substrate (TYR) was quantified after LPS/IFN-γ-stimulated cells were treated with NIL for 24 hr (left). Similarly, MAO activity in LPS/IFN-γ-stimulated and non-stimulated cells was examined with increasing concentrations of the substrate (right). The data indicate that neither iNOS protein expression nor NO_2^- has an effect on MAO activity. To confirm that TYR or DA inhibition of iNOS in LPS/IFN-γ-stimulated cells was not dependent upon MAO end products, we repeated the experiment in Fig. 1 in the presence or absence of the MAO-A and MAO-B inhibitors deprenyl and clorgyline (Fig. 7). Inhibition of MAO had little effect on the potency of TYR or DA to attenuate iNOS. Therefore, it appears that

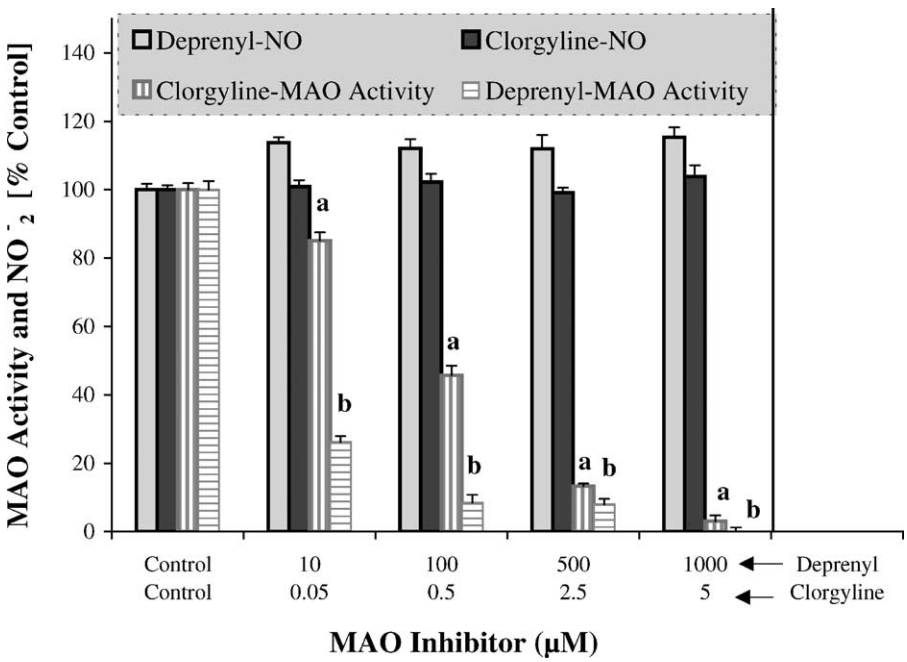

Fig. 4. Effect of MAO inhibitors on MAO and NO_2^- in LPS/IFN-γ-stimulated C6 glioma cells. Data represent MAO activity or NO_2^- produced [% control] and are expressed as means ± SEM, N = 4. Significance of difference from the control was determined by a one-way ANOVA, followed by a Tukey mean comparison post hoc test (clorgyline). Key: (a) $P < 0.001$ (deprenyl), (b) $P < 0.001$.

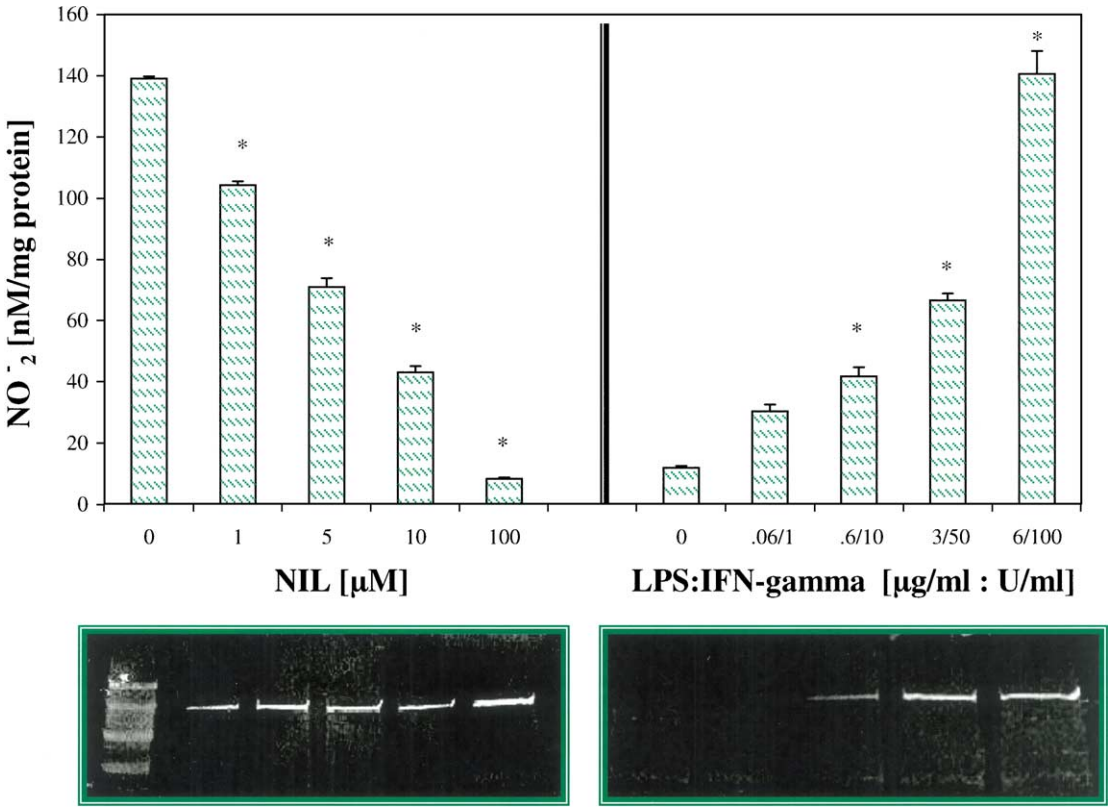

Fig. 5. Effect of NIL and LPS/IFN-γ on NO_2^- and iNOS protein expression. Data represent NO_2^- [nM/mg protein], and are expressed as means ± SEM, N = 4. Significance of difference from the control was determined by a one-way ANOVA, followed by a Tukey mean comparison post hoc test Key: (*) $P < 0.001$. Western blot analysis of iNOS is displayed below the charted data.

the ability of TYR and DA to attenuate iNOS is based on a unique chemical or structural property of these compounds. There is evidence to support the hypothesis that neurotransmitter receptors are located on astrocytes, and DA may exert iNOS inhibition through a receptor-mediated adenosine cAMP cascade. Recently, previous research in our laboratory has discovered that DA exerts effects on iNOS through activation of adrenergic rather

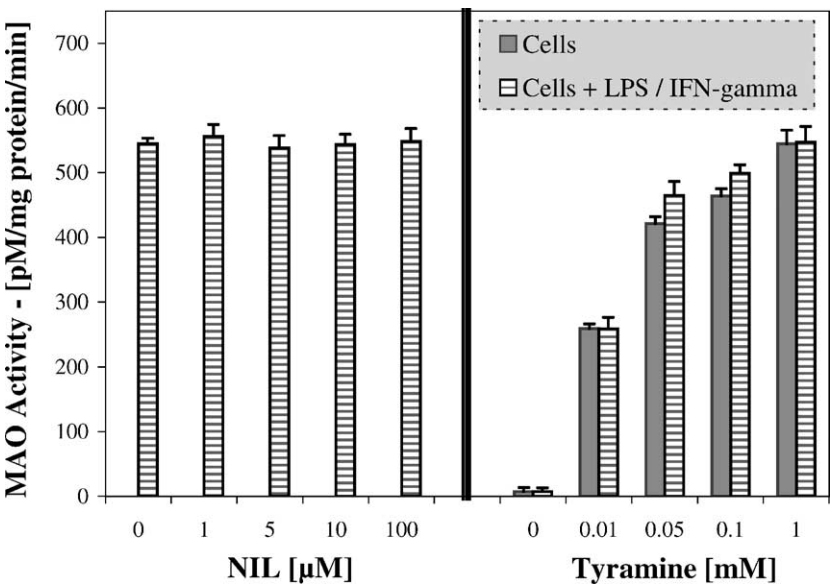

Fig. 6. Effect of iNOS protein expression and NO_2^- on MAO activity in LPS/IFN-γ-stimulated cells. Data represent MAO enzyme activity with various concentrations of NIL or TYR ± LPS/IFN-γ (6 μg/mL:100 U/mL). Data are expressed as means ± SEM, N = 4. Significance of difference from the control was determined by a one-way ANOVA, followed by a Tukey mean comparison post hoc test. Significance of difference between MAO activity in LPS/IFN-γ-treated cells and basal cells was determined by a two-way ANOVA (NS).

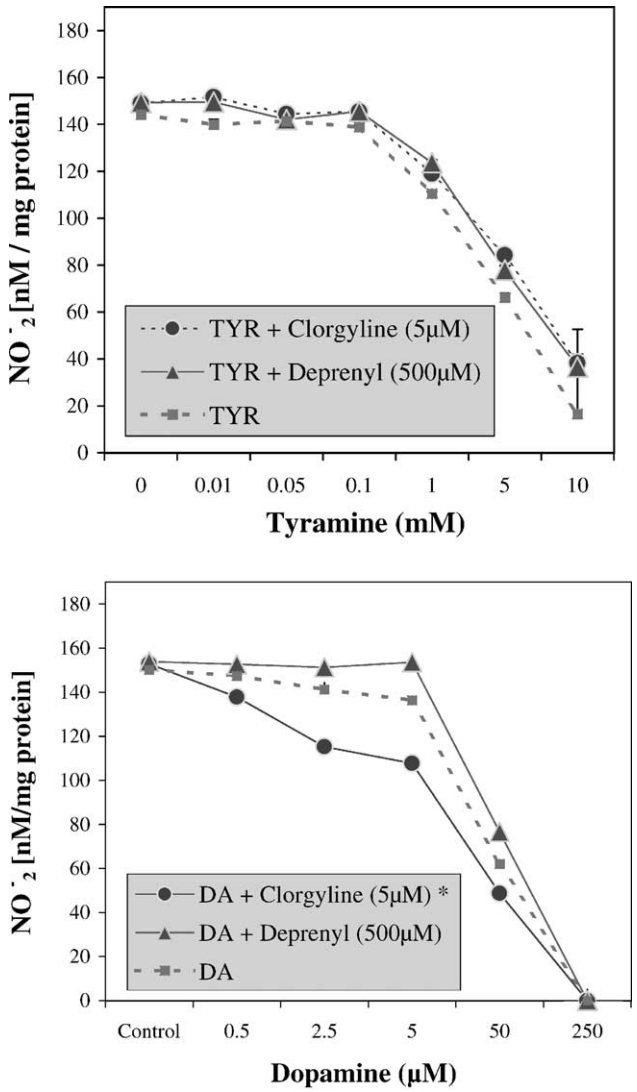

Fig. 7. Effects of deprenyl and clorgyline on TYR (top panel) and DA (bottom panel) attenuation of iNOS. Data represent NO_2^- [nM/mg protein], and are expressed as the means ± SEM, N = 4. Significance of difference from the DA or TYR control was determined by a two-way ANOVA. Key: (*) $P < 0.001$, DA + clorgyline values versus DA control.

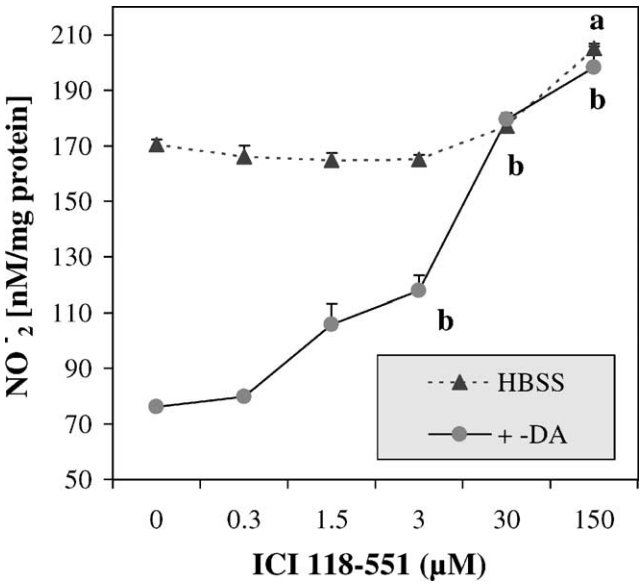

Fig. 8. Effect of ICI 118-551, a β_2-adrenergic antagonist, on iNOS attenuation by DA (175 μM). Data represent NO_2^- [nM/mg protein], and are expressed as means ± SEM, N = 4. Significance of difference from the DA or HBSS control was determined by a one-way ANOVA, followed by a Tukey mean comparison post hoc test. Key: (HBSS control) (a) $P < 0.001$ (DA), (b) $P < 0.001$.

than DA_1 or $DA_{2/3}$ receptors [31]. Figure 8 displays data regarding the effects of ICI 118-551, a β_2-adrenergic antagonist, on DA (175 μM) inhibition of NO_2^- in LPS/IFN-γ-treated cells. Unlike MAO inhibitors, blocking the β_2-adrenergic receptor completely prevented the inhibitory effects of DA on iNOS. From these data, we conclude that there is no defined relationship between iNOS and MAO in activated rat glioma cells. Moreover, the effects of DA are not mediated through MAO, but rather through an apparent receptor-mediated cascade.

4. Discussion

LPS is an antigenic component of the outer cell wall of Gram-negative *E. coli* bacteria, and is used to elicit a variety of inflammatory responses in animals. Similarly, transcriptional activation of iNOS in astrocytes is regulated by LPS in combination with various proinflammatory cytokines [3]. The data in this study provide preliminary evidence to suggest a lack of correlation between LPS/cytokine induction of iNOS and MAO activity in glioma cells. This conclusion is based on: (a) a high concentration of NO_2^- and iNOS protein having no effect on MAO activity; (b) MAO inhibition having no effect on NO_2^- in LPS/IFN-γ-stimulated cells; and (c) there being no noted difference in iNOS activity between groups with MAO substrates ± MAO inhibitors. This study was initiated because previous research in our laboratory has reported that several catecholamines, such as DA and norepinephrine, down-regulate NOS in a variety of cell lines including macrophages, neuroblastoma, and glioma (data not published). Similarly, catecholamines are also substrates for MAO. Further, this cell line was adequate to examine this relationship because substantial levels of both MAO and iNOS have been detected, specifically in C6 glioma cells [32,33].

An acute CNS inflammatory response in astrocytes may largely involve cytokine-activated changes in iNOS transcription, with little to no effects on MAO. On the other hand, elevated MAO-B protein levels and activity have been implicated in chronic rather than acute pathological conditions such as PD, AD, and Huntington's disease [34,35]. Evidence suggests a parallel relationship between elevation of brain MAO activity, and augmented vulnerability to age-related neurological degenerative disorders. Moreover, evidence from human brain postmortem studies

indicate that an age-related up-regulation of MAO-B juxtaposes the loss of CNS neurons [4]. Interestingly, epidemiological research reports a strong inverse correlation between cigarette smoking and risk for PD and AD [36]. And, cigarette smoke is a well-known potent inhibitor of both brain MAO-A and MAO-B [37]. These studies imply an extremely important role for MAO in the progressive vulnerability of neurodegenerative age-related diseases. It is thought that endogenous amine-related toxic compounds generated by MAO activity, such as *N*-Me-norsalsolinol and 1-benzyl-tetrahydroisoquinoline, play a contributing role in the etiology of chronic neurodegenerative pathologies [38]. The effective use of MAO inhibitors to provide protection against several experimental models of brain injury may be the result of conversion blockade of a precursor to its active neurotoxic metabolite, or unique chemical properties of the MAO inhibitor itself.

While little data have been derived on the effects of MAO on iNOS, it was reported recently that deprenyl can stimulate NO production through eNOS, accounting for observed potentiation of vasodilatatory responses in cerebral blood vessels [39]. While there appears to be a lack of relation between iNOS and MAO in glia, it is interesting to note that catecholamines (MAO substrates) exert direct inhibitory effects on iNOS protein expression in a variety of cell models, including macrophages and glia [24,40]. Moreover, there is significant evidence to support that human astrocytes contain D_1-, β_1-, and β_2-adrenergic receptors and A_2 adenosine receptors that are coupled to guanine nucleotide-binding protein (G_s) regulated adenylate cyclase-mediated intracellular signaling pathways [41]. Astrocytic iNOS mRNA is regulated by adenylate cyclase activity or intracellular levels of cAMP [42,43]. Therefore, it appears that the observed effects of catecholaminergic signal response in glial cells may occur through the elevation of cAMP and the subsequent suppression of iNOS protein expression [24]. In addition, similar to the findings in this study, there is evidence to suggest that DA exerts its primary effect through the cAMP-mediated β-adrenergic receptor cascade in glia [31,42].

While NO is thought to be a toxic and contributing component to CNS disease, it is interesting that there is a reduction of NO in the cerebral spinal fluid of PD, AD, and multiple system atrophy patients [44]. Moreover, under some conditions, NO has potent neuroprotective properties with the ability to potentiate neurotrophins and glutathione expression, and to act as an antioxidant against iron-mediated dopaminergic toxicity of the substantia nigra [45]. NO donors such as diethanolamine can attenuate free radical formation in glia and attenuate brain injury from ischemia/reperfusion [46,47]. It is plausible that the lack of NO may introduce an aspect of vulnerability in catecholaminergic neurons to degenerate.

In conclusion, while this study excludes a role for DA on iNOS transcription through MAO, it is likely that DA exerts its effects through a receptor-mediated signaling cascade. Future research will be required to determine the local signaling effects of DA on astrocytes *in vivo*, and to analyze if these effects participate in increased vulnerability of catecholaminergic neurons to degenerate in diseases of aging in the human brain.

Acknowledgments

This work was supported by grants received from the National Institutes of Health (NCRR 03020 and GM 08111).

References

[1] O'Kusky J, Colonnier M. A laminar analysis of the number of neurons, glia, and synapses in the adult cortex (area 17) of adult macaque monkeys. J Comp Neurol 1982;210:278–90.
[2] Squires RF. Discovery of monoamine oxidase forms A and B. Vopr Med Khim 1997;43:433–9.
[3] Wiesinger H. Arginine metabolism and the synthesis of nitric oxide in the nervous system. Prog Neurobiol 2001;64:365–91.
[4] Fowler JS, Volkow ND, Wang GJ, Logan J, Pappas N, Shea C, MacGregor R. Age-related increases in brain monoamine oxidase B in living healthy human subjects. Neurobiol Aging 1997;18:431–5.
[5] Bagasra O, Michaels FH, Zheng YM, Bobroski LE, Spitsin SV, Fu ZF, Tawadros R, Koprowski H. Activation of the inducible form of nitric oxide synthase in the brains of patients with multiple sclerosis. Proc Natl Acad Sci USA 1995;92:12041–5.
[6] Cesura AM, Pletscher A. The new generation of monoamine oxidase inhibitors. Prog Drug Res 1992;38:171–297.
[7] Skorobogataia TG. Substrate specificity of monoamine oxidase from the brain and liver of the human fetus during antenatal ontogenesis. Ukr Biokhim Zh 1986;58:81–3.
[8] Bredt DS, Snyder SH. Nitric oxide, a novel neuronal messenger. Neuron 1992;8:3–11.
[9] Bruhwyler J, Chleide E, Liegeois JF, Carreer F. Nitric oxide: a new messenger in the brain. Neurosci Biobehav Rev 1993;17:373–84.
[10] Zou MH, Daiber A, Peterson JA, Shoun H, Ullrich V. Rapid reactions of peroxynitrite with heme-thiolate proteins as the basis for protection of prostacyclin synthase from inactivation by nitration. Arch Biochem Biophys 2000;376:149–55.
[11] Molina y Vedia L, McDonald B, Reep B, Brüne B, DiSilvio M, Billiar TR, Lapetina EG. Nitric oxide-induced *S*-nitrosylation of glyceraldehyde-3-phosphate dehydrogenase inhibits enzymatic activity and increases endogenous ADP-ribosylation. J Biol Chem 1997;267:24929–32.
[12] Lizasoain I, Moro MA, Knowles RG, Darley-Usmar V, Moncada S. Nitric oxide and peroxynitrite exert distinct effects on mitochondrial respiration which are differentially blocked by glutathione or glucose. Biochem J 1996;314:877–80.
[13] Meyerson LR, McMurtrey KD, Davis VE. A rapid and sensitive potentiometric assay for monoamine oxidase using an ammonia-selective electrode. Anal Biochem 1978;86:287–97.
[14] Bartolini B, Tipton KF, Bianchi L, Stephenson D, Cunningham C, Della Corte L. Determination of monoamine oxidase activity by HPLC with fluorimetric detection. Neurobiology 1999;7:109–21.
[15] Pizzinat N, Copin N, Vindis C, Parini A, Cambon C. Reactive oxygen species production by monoamine oxidases in intact cells. Naunyn Schmiedebergs Arch Pharmacol 1999;359:428–31.
[16] Youdim MB, Lavie L. Selective MAO-A and B inhibitors, radical scavengers and nitric oxide synthase inhibitors in Parkinson's disease. Life Sci 1994;55:2077–82.

[17] Venarucci D, Venarucci V, Vallese A, Battila L, Casado A, De la Torre R, Lopez Fernandez ME. Free radicals: important cause of pathologies refer to ageing. Panminerva Med 1999;41:335–9.
[18] Li SW, Lin TS, Minteer S, Burke WJ. 3,4-Dihydroxyphenylacetaldehyde and hydrogen peroxide generate a hydroxyl radical: possible role in Parkinson's disease pathogenesis. Brain Res Mol Brain Res 2001;93:1–7.
[19] Burke WJ, Kristal BS, Yu BP, Li SW, Lin TS. Norepinephrine transmitter metabolite generates free radicals and activates mitochondrial permeability transition: a mechanism for DOPEGAL-induced apoptosis. Brain Res 1998;787:328–32.
[20] Tabner BJ, Turnbull S, El-Agnaf OM, Allsop D. Formation of hydrogen peroxide and hydroxyl radicals from Aβ and α-synuclein as a possible mechanism of cell death in Alzheimer's disease and Parkinson's disease. Free Radic Biol Med 2002;32:1076–83.
[21] Kristal BS, Conway AD, Brown AM, Jain JC, Ulluci PA, Li SW, Burke WJ. Selective dopaminergic vulnerability: 3,4-dihydroxyphenylacetaldehyde targets mitochondria. Free Radic Biol Med 2001;30: 924–31.
[22] Naoi M, Maruyama W, Takahashi T, Akao Y, Nakagawa Y. Involvement of endogenous *N*-methyl(*R*)salsolinol in Parkinson's disease: induction of apoptosis and protection by (−)deprenyl. J Neural Transm Suppl 2000;58:111–21.
[23] Law A, Gauthier S, Quirion R. Neuroprotective and neurorescuing effects of isoform-specific nitric oxide synthase inhibitors, nitric oxide scavenger, and antioxidant against beta-amyloid toxicity. Br J Pharmacol 2001;133:1114–24.
[24] Feinstein DL. Suppression of astroglial nitric oxide synthase expression by norepinephrine results from decreased NOS-2 promoter activity. J Neurochem 1998;70:1484–96.
[25] Miller KJ, Mariano CL, Cruz WR. Serotonin $5HT_{2A}$ receptor activation inhibits inducible nitric oxide synthase activity in C6 glioma cells. Life Sci 1997;61:1819–27.
[26] Holt A, Sharman DF, Baker GB, Palcic MM. A continuous spectrophotometric assay for monoamine oxidase and related enzymes in tissue homogenates. Anal Biochem 1997;244:384–92.
[27] Lowry OH, Rosebrough NJ, Farr AL, Randall RJ. Protein measurement with the Folin phenol reagent. J Biol Chem 1951;193:265–75.
[28] Park SK, Murphy S. Duration of expression of inducible nitric oxide synthase in glial cells. J Neurosci Res 1994;39:405–11.
[29] Evans SM, Casartelli A, Herreros E, Minnick DT, Day C, George E, Westmoreland C. Development of a high throughput in vitro toxicity screen predictive of high acute in vivo toxic potential. Toxicol In Vitro 2001;15:579–84.
[30] Chandler LJ, Kopnisky K, Richards E, Crews FT, Sumners C. Angiotensin II decreases inducible nitric oxide synthase expression in rat astroglial cultures. Am J Physiol 1995;268:C700–7.
[31] Mazzio E, Becker A, Soliman KFA. Characterization of neurotransmitters and dopamine on attenuation of inducible nitric oxide synthase in glioma cells. J Neuroimmunol 2002;131:70–82.
[32] Feinstein DL, Galea E, Roberts S, Berquist H, Wang H, Reis DJ. Induction of nitric oxide synthase in rat C6 glioma cells. J Neurochem 1994;62:315–21.
[33] Cawthon RM, Breakefield XO. Differences in the structures of monoamine oxidases A and B in rat clonal cell lines. Biochem Pharmacol 1983;32:441–8.
[34] Oreland L, Gottfries CG. Brain and brain monoamine oxidase in aging and in dementia of Alzheimer's type. Prog Neuropsychopharmacol Biol Psychiatry 1986;10:533–40.
[35] Hotamisligil GS, Girmen AS, Fink JS, Tivol E, Shalish C, Trofatter J, Baenziger J, Diamond S, Markham C, Sullivan J. Hereditary variations in monoamine oxidase as a risk factor for Parkinson's disease. Mov Disord 1994;9:305–10.
[36] Fratiglioni L, Wang HX. Smoking and Parkinson's and Alzheimer's disease: review of the epidemiological studies. Behav Brain Res 2000;113:117–20.
[37] Fowler JS, Volkow ND, Wang GJ, Pappas N, Logan J, Shea C, Alexoff D, MacGregor RR, Schlyer DJ, Zezulkova I, Wolf AP. Brain monoamine oxidase A inhibition in cigarette smokers. Proc Natl Acad Sci USA 1996;93:14065–9.
[38] Kotake Y, Tasaki Y, Makino Y, Ohta S, Hirobe M. 1-Benzyl-1,2,3,4-tetrahydroisoquinoline as a parkinsonism-inducing agent: a novel endogenous amine in mouse brain and parkinsonian CSF. J Neurochem 1995;65:2633–8.
[39] Thomas T, McLendon C, Thomas G. L-Deprenyl: nitric oxide production and dilation of cerebral blood vessels. Neuroreport 1998;9:2595–600.
[40] Boomershine CS, Lafuse WP, Zwilling BS. β2-Adrenergic receptor stimulation inhibits nitric oxide generation by *Mycobacterium avium* infected macrophages. J Neuroimmunol 1999;101:68–75.
[41] Porter JT, McCarthy KD. Astrocytic neurotransmitter receptors *in situ* and *in vivo*. Prog Neurobiol 1997;51:439–55.
[42] Chang JY, Liu LZ. Catecholamines inhibit microglial nitric oxide production. Brain Res Bull 2000;52:525–30.
[43] Pahan K, Namboodiri AM, Sheikh FG, Smith BT, Singh I. Increasing cAMP attenuates induction of inducible nitric-oxide synthase in rat primary astrocytes. J Biol Chem 1997;272:7786–91.
[44] Kuiper MA, Visser JJ, Bergmans PL, Scheltens P, Wolters EC. Decreased cerebrospinal fluid nitrate levels in Parkinson's disease, Alzheimer's disease and multiple system atrophy patients. J Neurol Sci 1994;121:46–9.
[45] Rauhala P, Mohanakumar KP, Sziraki I, Lin AM, Chiueh CC. *S*-Nitrosothiols and nitric oxide, but not sodium nitroprusside, protect nigrostriatal dopamine neurons against iron-induced oxidative stress in vivo. Synapse 1996;23:58–60.
[46] Dobrucki LW, Kalinowski L, Uracz W, Malinski T. The protective role of nitric oxide in the brain ischemia. J Physiol Pharmacol 2000;51: 695–703.
[47] Mason RB, Pluta RM, Walbridge S, Wink DA, Oldfield EH, Boock RJ. Production of reactive oxygen species after reperfusion in vitro and in vivo: protective effect of nitric oxide. J Neurosurg 2000;93:99–107.